Hindawi
Journal of Food Biochemistry
Volume 2023, Article ID 7729962, 11 pages
https://doi.org/10.1155/2023/7729962

Research Article

Ursolic Acid Inhibits the Growth of Gastric Cancer by Targeting KLF4/YAP1

Fenfen Xiang, Mengzhe Zhang, Wenbin Hao, Rongrong Liu, Qian Li, Qing Gu, Zhaowei Zhu, Zixi Chen, Xiaoxiao Li, Xiangdong Kang, and Rong Wu

Laboratory Medicine, Putuo Hospital, Shanghai University of Traditional Chinese Medicine, Shanghai 200062, China

Correspondence should be addressed to Xiangdong Kang; xd_kang@163.com and Rong Wu; rong701@126.com

Received 6 April 2023; Revised 4 July 2023; Accepted 17 July 2023; Published 11 August 2023

Academic Editor: Muhammad Sajid Arshad

Krüppel-like factor 4 (KLF4) is a zinc-finger transcription factor which has various mechanisms in different tumors. Ursolic acid (UA), a natural compound that exists in many herbs, is known to prevent tumor progression and has anticancer effects on many human cancers. The present study was to evaluate the antitumor effect of UA on gastric cancer (GC) through KLF4 and the Hippo pathway. Our data showed that UA inhibited the growth of GC *in vivo* and *in vitro*. UA treatment significantly increased the expression of KLF4 and decreased the expression of CTGF. The overexpression of KLF4 inhibited the proliferation and cell cycle of GC and decreased the expression of CTGF, whereas the knockdown of KLF4 attenuated the effects of UA. Furthermore, the inhibition of CTGF arrested tumor cells in G2/M which blocked proliferation progress. Confocal laser scanning and molecular simulation software MOE showed that KLF4 combined with YAP1 which may block the formation of the TEADs-YAP1 complex to interrupt the expression of CTGF and the downstream oncogenic process. In conclusion, UA can inhibit GC growth both *in vivo* and *in vitro*, and it activated KLF4 which may competitively bind with YAP1 against TEADs and block the oncogenic Hippo pathways.

1. Introduction

GC is the fifth most common malignancy worldwide, and it is the third most frequent cause of cancer-related death with a high incidence rate [1, 2]. Though emerging advances in biological and surgical therapy have improved the cure rate of GC patients, there was no notable improvement in overall survival partly [3, 4]. Therefore, it is necessary to find the molecular basis of GC tumorigenesis and progression to obtain improved clinical results for GC patients.

Krüppel-like factor 4 (KLF4) is a zinc-finger transcription factor and has three zinc-finger domains in its C-terminus, and one of its zinc-finger domains contains a "PPGF" motif. KLF4 is a potential tumor suppressor in gastrointestinal cancers [5, 6]. Decreased expression of KLF4 was found in gastrointestinal epithelial tumors [7] and esophageal squamous cell carcinoma patients [8]. The absence of KLF4 enhanced the occurrence of GC, while the overexpression of KLF4 reduced cancer colony formation, migration, and invasion [9]. Furthermore, KLF4 was reported to inhibit the expression of a typical target gene of YAP1 named CTGF [10]. Our preliminary work showed that expression of KLF4 is related to the proliferation of GC BGC-823 cells and that overexpression of KLF4 can inhibit the expression of CTGF. However, how KLF4 inhibits CTGF expression remains unknown.

Multiple pieces of evidence have uncovered the importance of the Hippo signaling pathway in gastric tumorigenesis [11, 12]. As the key downstream mediator of the Hippo pathway, YAP1, a transcriptional coactivator, is frequently activated in GC patients. The overexpression of nuclear YAP1 is related to a poor prognosis [13], whereas knockdown of YAP1 inhibits several stages of GC development such as cell proliferation, migration, invasion, and metastasis [14], suggesting that inhibition of YAP1 transcriptional activity may prevent tumor progression in GC. YAP1 locates in the nucleus where it binds with transcription factor TEADs and activates its transcription

process, thereby stimulating the expression of proliferative genes such as connective tissue growth factor (CTGF) [15]. Based on the fact that KLF4 contains a "PPGF" motif and can inhibit the expression of CTGF, we hypothesize that KLF4 may bind to YAP1 and hinder the binding of YAP1 to TEADs, which requires further experimental validation.

Natural plants provide an important source for obtaining novel therapeutic molecules for cancer treatment. UA is a promising natural compound for cancer prevention and therapy, and it has been demonstrated to possess a number of anticancer activities, including the inhibition of tumorigenesis, tumor promotion, and angiogenesis [16–18]. Our preliminary work showed that UA could inhibit the growth of GC cells and regulate the expression of KLF4, while the deepening mechanism remains unclear.

In the view of unsettled issues above, the aim of this study was to further elucidate the effects of UA on GC, and we emphatically investigated the interaction between KLF4 and YAP1. Our work demonstrated that UA could inhibit gastric tumorigenesis both *in vitro* and *in vivo*, and the inhibitory effects of UA were evaluated through KLF4 which competitively binds with YAP1 and negatively inhibits oncogenic gene CTGF.

2. Materials and Methods

2.1. Cell Culture and Reagents. Human GC cell line BCG-823 was obtained from the Central Laboratory of Putuo Hospital, Shanghai University of Traditional Chinese Medicine. The BCG-823 cells were maintained in RPMI 1640 medium (Hyclone, USA) containing 10% fetal bovine serum (FBS), 100 U/ml penicillin, and 100 g/ml streptomycin (Hyclone, USA). UA (Selleck, USA) was dissolved in dimethyl sulfoxide (DMSO, Sigma, USA) and stored at −20°C.

2.2. Cell Proliferation Assays. BCG-823 cells were harvested and adjusted to 1×10^4 cells/well and seeded in 96-well culture plates. The cells were treated with UA at different doses with triplicates at 37°C in a 5% CO_2 incubator. The cell proliferation assays were performed as previously reported [19].

2.3. Cell Cycle Analysis. Cells were collected by centrifuging for 5 min at 1,000 rpm, 4°C and resuspended in cold PBS. Then, 100 μl of 200 μg/ml DNase-free RNaseA was added to cell suspension and incubated for 30 min at 37°C. The cells were stained with 100 μl of 1 mg/ml propidium iodide. After shaking, the cells were incubated in the darkness for 30 min. Flow cytometry was performed on BD FACS Calibur using BD CellQuest Pro software. Data were analyzed by using FlowJo software (Tree Star Inc., Ashland, USA).

2.4. Quantitative Real-Time PCR. Quantitative real-time PCR was performed as previously reported [20]. The expression levels of genes were normalized to GAPDH. The primers of genes are listed in Table 1.

2.5. Western Blot Analysis. Equal amounts of protein were loaded and separated discontinuously on 12% sodium dodecyl sulfate-polyacrylamide (SDS-PAGE) gels and subsequently transferred onto a nitrocellulose membrane (Amersham Pharmacia, UK). The membrane was then incubated in TBST blocking solution (Tris-buffered saline including 0.1% Tween 20) containing 5% skim milk for 2 h at room temperature, followed by separate incubation with primary antibodies against KLF4, CTGF, Akt and p-Akt (CST), and β-actin (Beyotime, Jiangsu, China) overnight at 4°C. After washing, the membrane was incubated with respective secondary antibodies for 2 h. Immunoblot was detected with enhanced chemiluminescence (Pierce Biotechnology) according to the manufacturer's instructions.

2.6. Immunofluorescent Staining. The cells were collected in microcentrifuge tubes and washed with PBS 3 times. The cells were immobilized with immunol staining fix solution (Beyotime, China) for 20 min and washed with PBS 3 times. The cells were blocked with 5% BSA solution containing 0.1% Triton-X 100 for 40 min at room temperature and then incubated at 4°C overnight in the same solution containing the antibody. After incubation, the cells were washed with PBS 3 times and incubated with anti-mouse FITC-IgG (BD Biosciences, USA) at 37°C for 2 h. After wash, the cells were stained with DAPI for 5 min, and the images were acquired by using a fluorescence microscope (Leica, Germany).

2.7. Gold Yeast Two-Hybrid System. The Matchmaker™ Gold Yeast two-hybrid system (Clontech) was used according to the manufacturer's instructions. To screen protein-protein interactions, respective bait (pGBKT7) and prey (pGADT7) plasmids were cotransformed into the yeast strain Y2HGold (Clontech), and cotransformants were selected on high-stringency double dropout (DDO) and quadruple dropout (QDO) plates containing 0.04 mg/ml 5-bromo-4-chloro-3-indolyl-d-galactopyranoside (X-α-Gal) and 0.2 μg/ml Aureobasidin A (ABA). Double dropout plates were designed as SD/-Trp/-Leu/AbA/X-α-gal, and quadruple dropout plates were designed as SD/-Trp/-Leu/-His/-Ade/AbA/X-α-gal.

2.8. Homology Modeling. The target sequence of KLF4 was obtained from UniProt, with the UniProt ID of Q6TH77. Template crystal structures were identified through BLAST and downloaded from RCSB Protein Data Bank (PDB ID: 2WBU). Homology modeling was conducted in MOEv2015. The protonation state of the protein and the orientation of hydrogens were optimized by using LigX, at a pH of 7 and a temperature of 300 K. First, the target sequence was aligned to the template sequence, and ten independent intermediate models were built. These different homology models were the result of the permutational selection of different loop candidates and side-chain rotamers. Then, the intermediate model that scored best according to the GB/VI scoring function was chosen as the final model, subject to further energy minimization using the AMBER12/EHT force field.

Table 1: Nucleotide sequences of primers used for qRT-PCR reactions.

Genes	Forward	Reverse
KLF4	5′-CGGAGAGAGACCGAGGAGTT-3′	5′-AAGAGGAGGCTGACGCTGA-3′
CTGF	5′-TACCAATGACAACGCCTCCT-3′	5′-TTGGGAGTACGGATGCACTT-3′
P21	5′-CGACTGTGATGCGCTAATGG-3′	5′-CTCCAGTGGTGTCTCGGTGA-3′
P27	5′-GCTCCGGCTAACTCTGAGGA-3′	5′-AAGAATCGTCGGTTGCAGGT-3′
Gli2	5′-GAGCCATCAAGACCGAGAGC-3′	5′-CATCTCCACGCCACTGTCAT-3′
GAPDH	5′-GAAGGTGAAGGTCGGAGTC-3′	5′-GAAGATGGTGATGGGATTTC-3′

2.9. Protein-Protein Docking. The protein-protein dock module in MOEv2015 was used for protein-protein docking simulations of KLF4 and YAP1. The 3D structure of KLF4 was predicted through homology modeling as mentioned before. The 3D structure of YAP1 was downloaded from RCSB Protein Data Bank (PDB ID: 4REX), which reported the crystal structure of the first WW domain of human YAP1, with a resolution of 1.6 Å. Then, the protonation state of the enzyme and the orientation of hydrogens were optimized by using LigX, at a pH of 7 and a temperature of 300 K. Prior to docking, the force field of AMBER12: EHT and the implicit solvation model of reaction field (R-field) were selected. KLF4 and YAP1 were defined as a receptor and ligand, respectively. The PPGF in KLF4 was selected and defined as a ligand site. The docking workflow followed the "induced fit" protocol, in which the side chains of the receptor pocket were allowed to move according to ligand conformations, with a constraint on their positions. The docked poses were refined with top 100 poses retained by a rescoring of GBVI/WSAdG. The detection and analysis were conducted by Shanghai PSI Biotechnology Co., Ltd.

2.10. Coimmunoprecipitation Assay. Lentivirus-containing human KLF4-Flag cDNA was designed and constructed by Genechem using lentiviral vector GV358 (Genechem, Shanghai, China). The BGC-823 cells with overexpression of KLF4 were harvested and lysed with IP lysis buffer (20 mM Tris pH 7.5, 150 mM NaCl, 1% TritonX-100, 1 mM EDTA, and protease inhibitors) and immunoprecipitated with anti-Flag magnetic beads overnight at 4°C to pull down KLF4 protein. These beads were washed three times with lysis buffer. After separation by SDS-PAGE, the immunoprecipitates were subjected to immunoblotting analysis with an anti-YAP antibody.

2.11. Orthotopic Tumor Transplantation Models and Treatments. Male athymic nude mice (6 weeks old) were purchased from the Shanghai Experimental Animal Center of Chinese Academic of Science (Shanghai, China). Mice were maintained under specific pathogen-free conditions in the animal facility of Putuo Hospital, Shanghai University of Traditional Chinese Medicine. The BCG-823 cells (1×10^6) were injected subcutaneously into the right flank of mice. Tumors were collected and cut into small pieces less than 1 mm^3 after the size of tumors was determined, and then, purse-string sutures were performed on the anterior wall of the stomach. These mice were randomly divided into 2 groups, 8 in each group, one group received UA (50 ug/g) for 8 weeks and the other group received DMSO. In addition, the BGC-823 cells infected with lentivirus encoding KLF4 (BGC-823-KLF4) and negative control (BGC-823-NC) were injected into the right flank of the mouse, 8 in each group. The body weight and the tumor volume of the mice were measured by using a caliper on the sacrificed day. All procedures were approved by the Animal Experimentation Ethics Committee of Putuo Hospital Affiliated to Shanghai University of Traditional Chinese Medicine.

2.12. Statistical Analysis. Data were analyzed for statistical significance using Student's *t*-test for the difference between two groups. All analyses were calculated by using GraphPad and SPSS 21.0 Software. $p < 0.05$ was considered statistically significant.

3. Results

3.1. Effects of UA on the Proliferation and Cell Cycle of GC BGC-823 Cells. To validate the inhibitory effects of UA on GC cells, we measured the proliferation of the BGC-823 cells which were treated with UA at various concentrations for 24 h. The data confirmed that UA inhibited the proliferation of the BGC-823 cells with effects proportional to incubation dosage, and the doses of IC50 of UA for 24 h were 52.75 μM in the BGC-823 cells (Figure 1(a)). As cell proliferation was significantly suppressed by UA at concentrations less than 50 μM, this dosage range was used in subsequent experiments.

To analyze how UA regulated the proliferation of the BGC-823 cells, DNA flow cytometric analysis was performed to determine the effect of UA on the cell cycle of the BGC-823 cells. We found that after treatment with UA, the S phase of cells decreased significantly and the G2/M phase increased (Figures 1(b) and 1(c)). Furthermore, we tested the protein level of P21 and P27, and it showed that the expression of P21 and P27 increased significantly after treatment with UA (Figure 1(d)). The results determined the effect of UA on the cell cycles of the BGC-823 cells.

3.2. UA Inhibited the Growth of GC BGC-823 Cells through Upregulation of KLF4. In our previous study, we found that KLF4 played an important role in inhibiting tumor growth, to explore whether UA inhibited GC growth by targeting KLF4 in the BGC-823 cells, we evaluated the effects of UA on the expression of KLF4, and the results showed that the mRNA and protein level of KLF4 in BGC-823 cells after treatment with UA increased significantly compared to those in the BGC-823 control cells

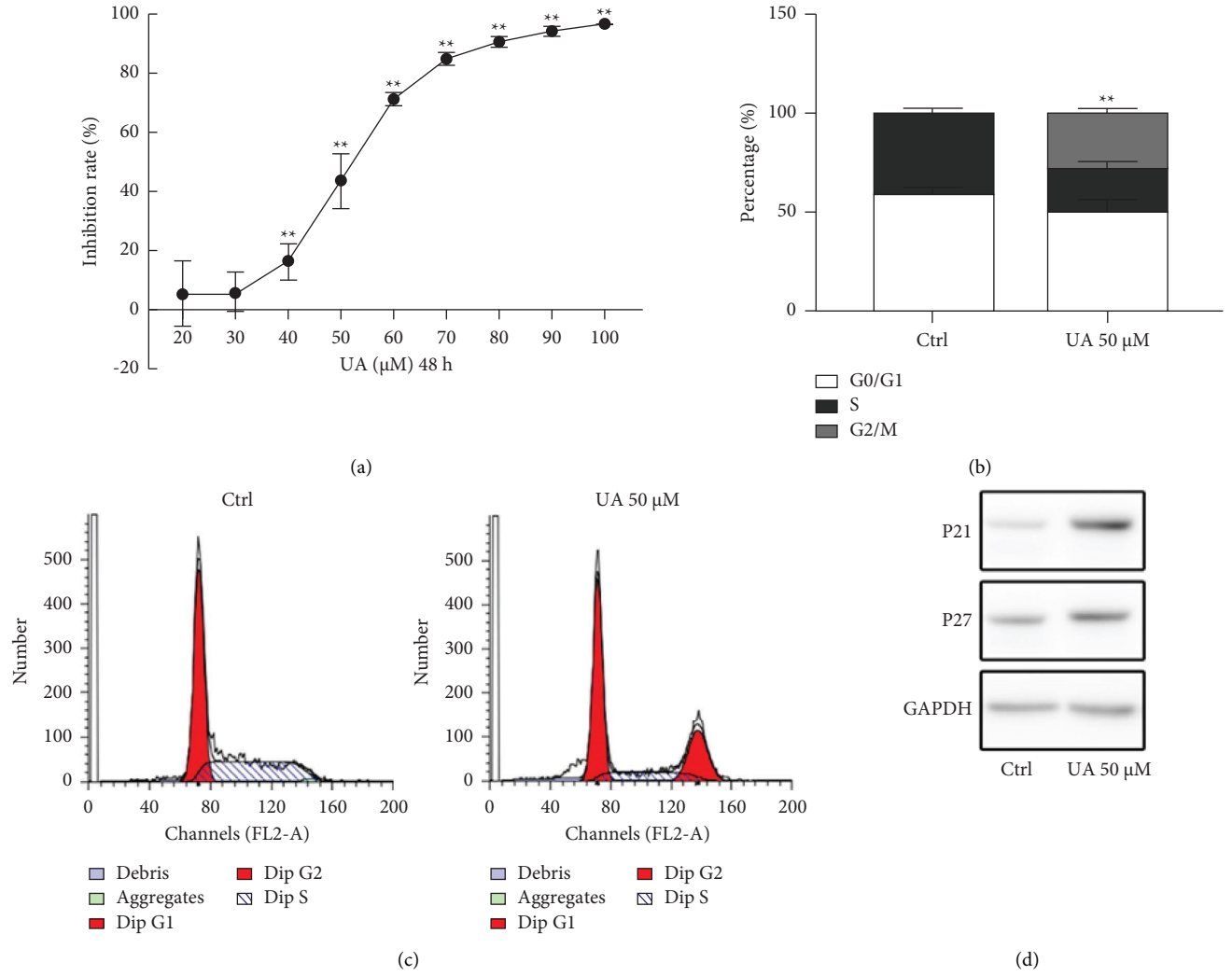

Figure 1: Effects of UA on the proliferation and cell cycle of GC BGC-823 cells. (a) The inhibition of cell proliferation by UA in BGC-823 cells. (b) G2/M and S-phase analysis of the cell cycle of BGC-823 cells treated with UA. (c) Flow cytometric analysis of the cell cycle of BGC-823 cells treated with UA. (d) Changes of P21 and P27 protein levels in BGC-823 cells after treatment with UA. $^{**}P < 0.01$ versus the control group.

(Figures 2(a) and 2(b)). Also, the expression of CTGF decreased, and the expression of P21 and P27 increased significantly (Figure 2(c)).

To confirm the efficacy of KLF4 in inhibiting GC cells, we used a lentivirus expressing KLF4 to achieve the overexpression of KLF4 in the BGC-823 cells. qRT-PCR and western blot analysis showed that the KLF4 level in the BGC-823 cells transfected with the KLF4 overexpression vector was notably higher than that in the BGC-823 control cells (Figure 2(d)). The proliferation of the BGC-823 cells with overexpression of KLF4 was significantly inhibited (Figure 2(e)). These results suggest that the overexpression of KLF4 could inhibit the growth of the BGC-823 cells.

To further verify the efficacy of UA in inhibiting the BGC-823 cells by targeting KLF4, we transfected the BGC-823 cells with a lentivirus to stably suppress KLF4 expression in the BGC-823 cells. qRT-PCR and western blot analysis showed that the KLF4 level significantly decreased in the BGC-823 cells transfected with the KLF4 lentivirus compared with the level in the BGC-823 control cells (Figure 2(f)). The CCK-8 results showed that the inhibition of BGC-823 cell proliferation in cells with lower KLF4 was decreased compared to that of the control cells after the UA treatment (Figure 2(g)). The results indicated that UA was unable to effectively inhibit the growth of the BGC-823 cells when the expression of KLF4 was suppressed. It was conceivable that UA inhibited the growth of the BGC-823 cells through the regulation of KLF4 expression.

3.3. KLF4 Inhibited the Growth of GC Cells through Down-regulation of CTGF. CTGF plays a key role in the regulation of cell growth; to assess whether KLF4 was involved in the regulation of CTGF expression in BGC-823 cells, we detected the expression level of CTGF by qRT-PCR analyses. As shown in Figure 3(a), the expression level of CTGF significantly decreased in the BGC-823 cells overexpressing

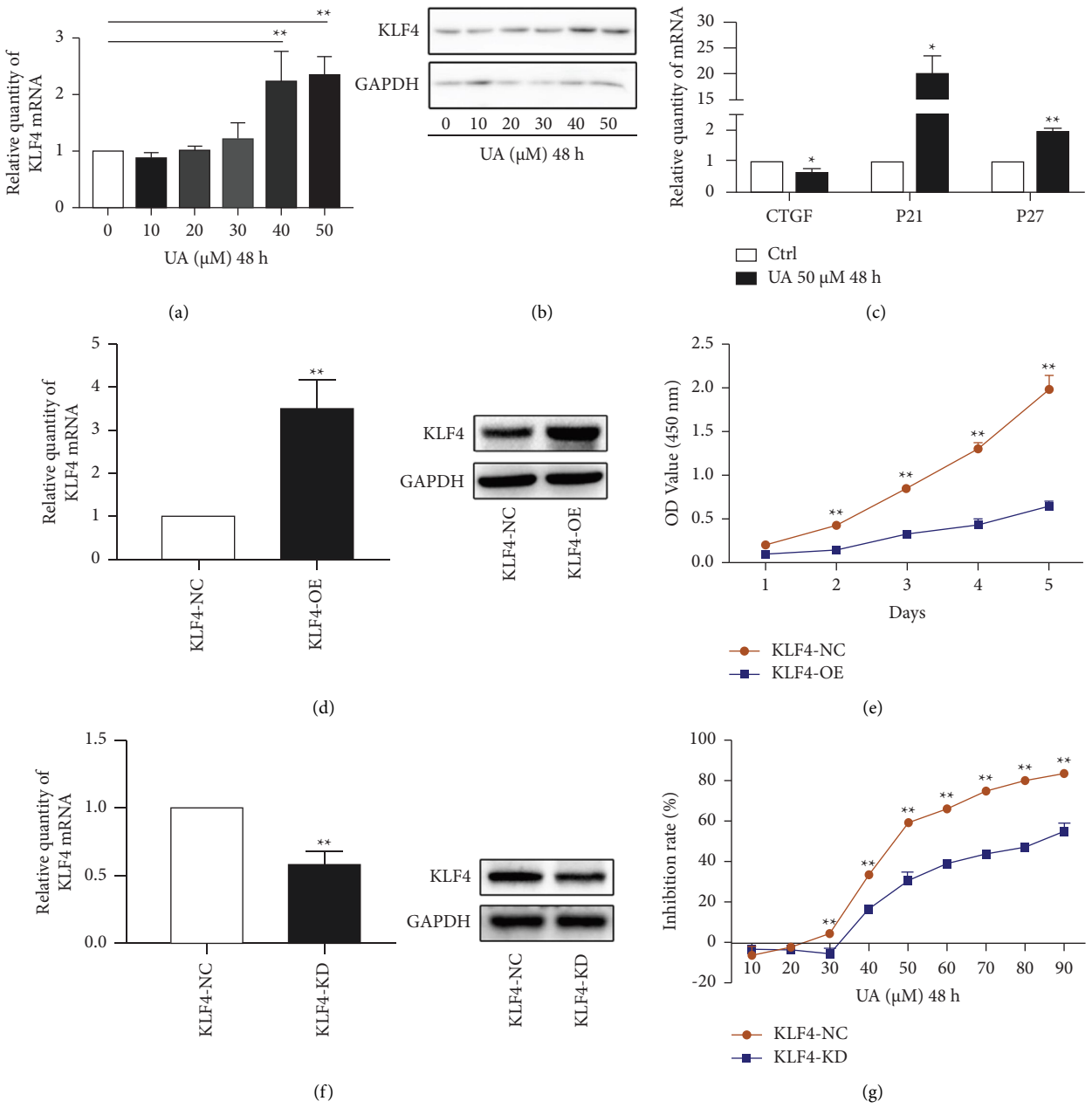

Figure 2: UA inhibited the growth of GC BGC-823 cells through upregulation of KLF4. (a) Changes of KLF4 mRNA levels in BGC-823 cells after treatment with UA. (b) Changes of KLF4 protein levels in BGC-823 cells after treatment with UA. (c) Changes of CTGF, P21, and P27 mRNA levels in BGC-823 cells after treatment with UA. (d) Real-time PCR and western blot analyses of KLF4 expression levels after transfection of the KLF4 overexpression lentivirus in BGC-823 cells. (e) The inhibition of cell proliferation in BGC-823 cells after overexpression of KLF4. (f) Real-time PCR and western blot analyses of KLF4 expression levels after transfection of KLF4 RNAi in BGC-823 cells. (g) The inhibition of cell proliferation in BGC-823 cells after downregulation of KLF4.

KLF4 compared to the expression level in the control cells. In addition, there was a significant increase in the P21 and P27 expression level (Figure 3(a)). The results were indicative of the ability of KLF4 to alter CTGF expression levels in the BGC-823 cells. To further verify the efficacy of CTGF in inhibiting the BGC-823 cells, we transfected the BGC-823 cells with a lentivirus to stably suppress CTGF expression in the BGC-823 cells. The CCK-8 results showed that the proliferation of the BGC-823 cell cells with lower CTGF decreased compared to that of the control cells (Figure 3(b)). DNA flow cytometric analysis showed that the G2/M phase increased when CTFG translation was blocked (Figures 3(c) and 3(d)). Furthermore, the downstream AKT signaling pathways genes such as P21 and P27 significantly increased with the downregulation of CTFG (Figures 3(e) and 3(f)). It is conceivable that UA inhibits the growth of the BGC-823 cells through the regulation of KLF4/CTGF expression.

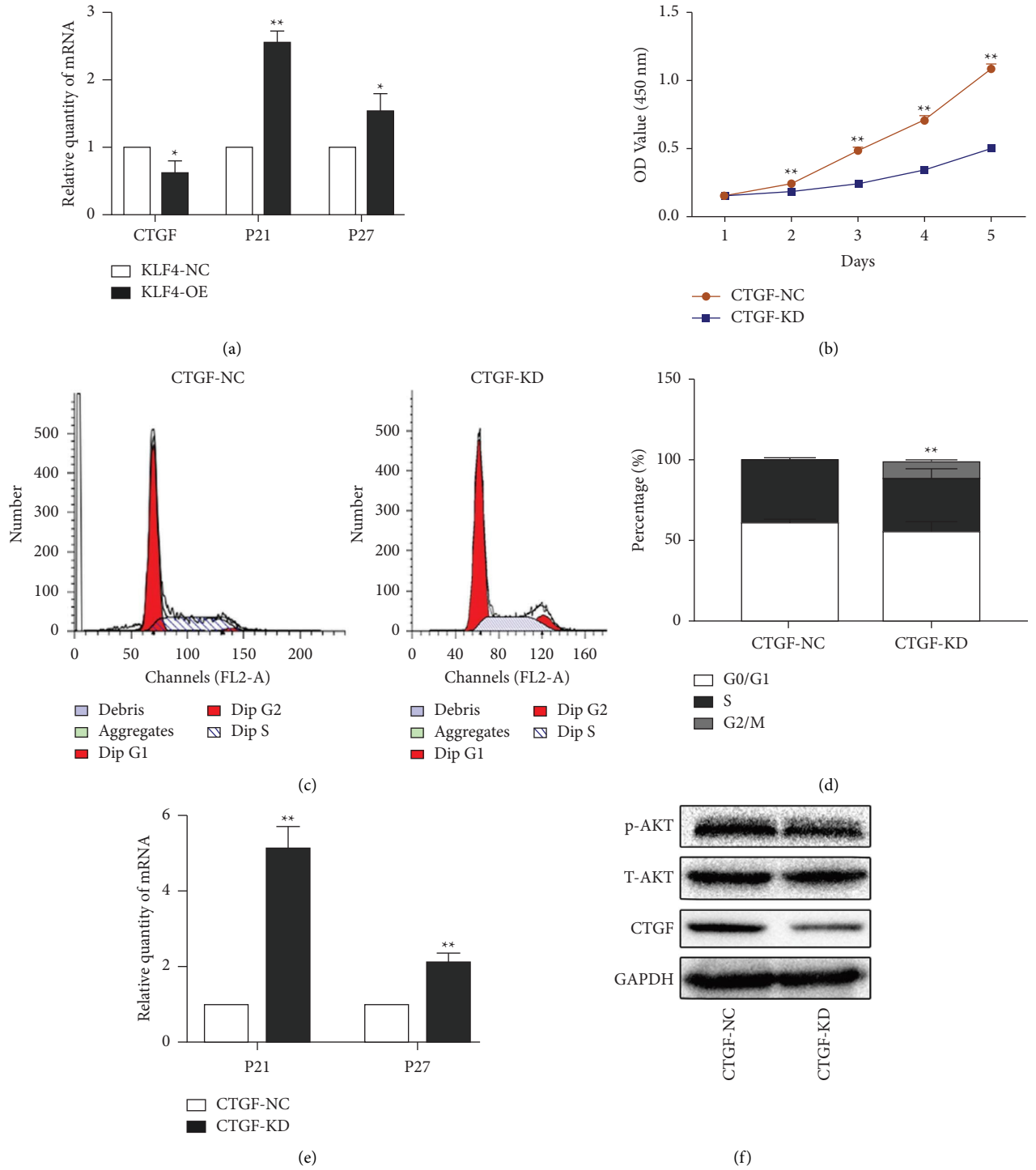

Figure 3: KLF4 inhibited the growth of GC cells through downregulation of CTGF. (a) Changes of CTGF, P21, and P27 mRNA levels in BGC-823 cells after overexpression of KLF4. (b) The inhibition of cell proliferation in BGC-823 cells after downregulation of CTGF. (c) Flow cytometric analysis of the cell cycle of BGC-823 cells after downregulation of CTGF. (d) G2/M and S-phase analysis of the cell cycle of BGC-823 cells after downregulation of CTGF. (e) Changes of P21 and P27 mRNA levels in BGC-823 cells after downregulation of CTGF. (f) Western blot analyses of p-AKT and CTGF expression levels after downregulation of CTGF.

3.4. KLF4 and TEADs Compete for Interaction with YAP1 Protein. Given that CTGF negatively correlated with KLF4, we tested whether KLF4 may physically interact with upstream YAP1. By performing immunofluorescent staining in the BCG-823 cells, we found hyperactivation of KLF4 may combine with YAP1 (Figure 4(a)). Subsequently, we demonstrated that YAP1 can interact with KLF4 and TEAD4 by using a yeast two-hybrid system (Figure 4(b)). Thus, we

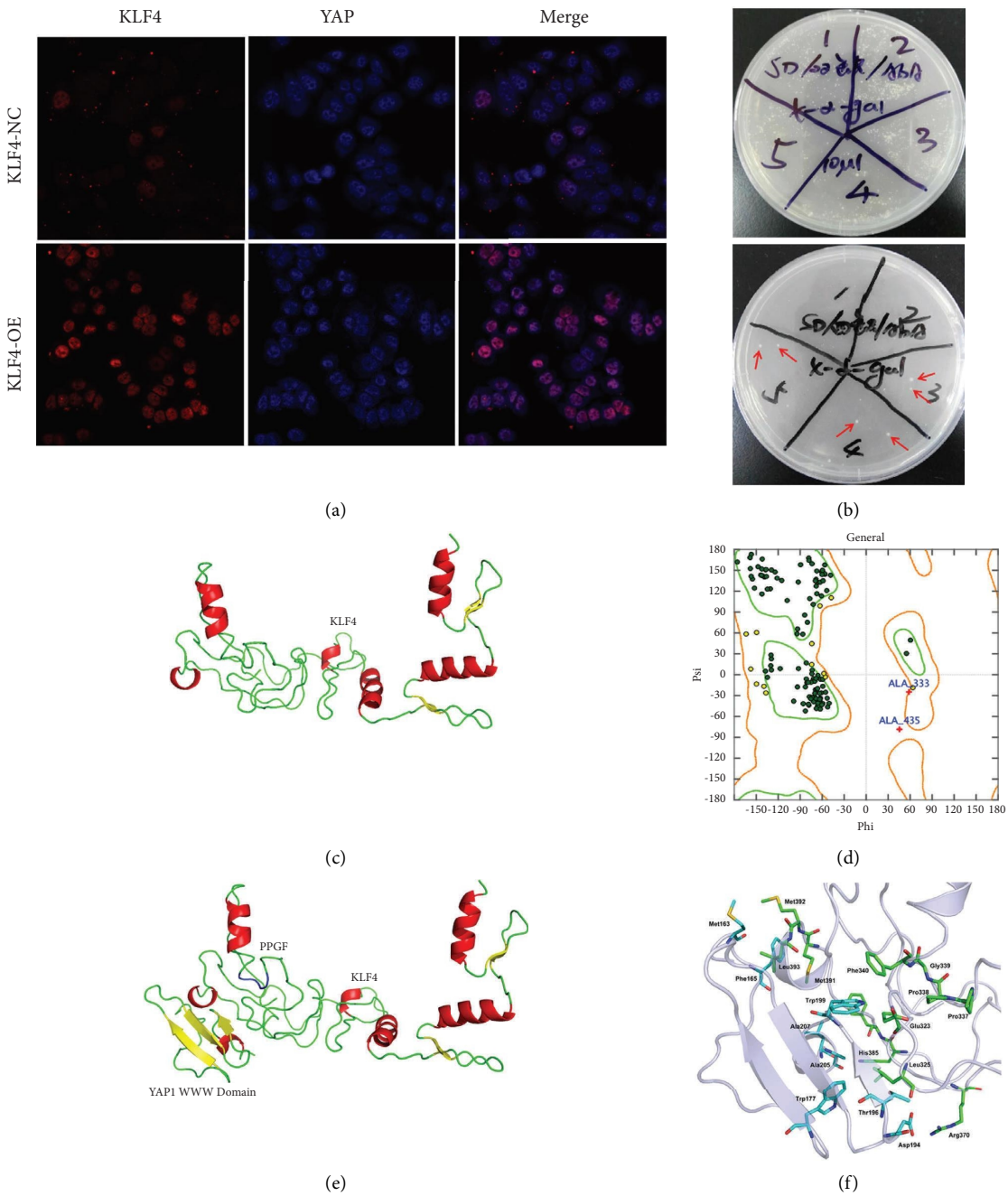

Figure 4: Continued.

Index	Type	Chain	Residue	Chain	Residue
1	HB	KLF4	GLU323.OE1	YAP1	TRP199.NE1
2	HB	KLF4	LEU325.0	YAP1	THR196.OG1
3	HB	KLF4	KLF4	YAP1	ASP194.OD1
4	HB	KLF4	KLF4	YAP1	ALA205.O
5	HYD	KLF4	LEU325.CD1	YAP1	TRP177.CZ2
6	HYD	KLF4	PHE340.CE2	YAP1	TRP199.CD1
7	HYD	KLF4	PHE386.CE2	YAP1	LEU207.CD1
8	HYD	KLF4	MET391.CB	YAP1	PHE165.CB
9	HYD	KLF4	MET392.CE	YAP1	MET163.CE
10	HYD	KLF4	LEU393.CD2	YAP1	MET163.CB
11	HYD	KLF4	LEU393.CD1	YAP1	PHE165.CB
12	ION	KLF4	ARG370.NH2	YAP1	ASP194.OD1

(g)

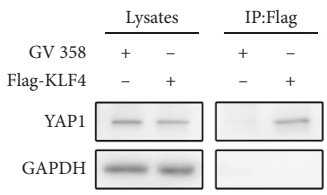

(h)

Figure 4: KLF4 and TEADs compete for interaction with YAP1 protein. (a) Cell immunofluorescence assay of KLF4 and YAP1 in BGC-823. (b) 1–5: yeast cotransformed with pgadt7 + pgbkt7 (blank control), pgadt7-t + pgbkt7-lam (negative control, large *t* antigen does not bind to lam protein), pgadt7-t + pgbkt7-P53 (positive control, large *t* antigen can bind to p53 protein), pgadt7-yap1 + pgbkt7-klf4 (experimental group 1), and pgadt7-yap1 + pgbkt7-tead4 (experimental group 2). Above: five groups of plasmid transfected Y2hgold were coated on the double deficient plate (SD/-Trp/-Leu/AbA/X-α-Gal), below: five groups of plasmids were transfected with Y2hgold and coated on the four deficient plates (SD/-Trp/-Leu/-His/-Ade/AbA/X-α-Gal). (c) The crystal model of KLF4. (d) The score of the KLF4 model according to the GB/VI score function. (e–g) The docking site between KLF4 and YAP1. (h) Co-IP assay indicated binding of KLF4 and YAP1 in BGC-823 cells.

speculated that KLF4 and TEAD4 competitively bind to YAP1, leading to reduced transcription of CTGF.

Furthermore, we calculated and analyzed the protein interaction sites between KLF4 and YAP1 using MOE 2015 docking software. The crystal model of KLF4 (Figure 4(c)) and the score of the KLF4 model (Figure 4(d)) are according to the GB/VI score function, where the dark green dots represent the residue of the most favorable region, the yellow dots represent the residues in the additional allowed area, and the small red crosses represent the residues in the prohibited area. Figure 4(e) represents the docking site between KLF4 and YAP1. The indole ring of Trp199 in the "WW" domain of YAP1 interacts with Phe340 in the "PPGF" sequence of KLF4 to form van der Waals and hydrophobic interactions. Trp199 also forms hydrogen bonds with the carboxyl group of Glu323. In addition, residues Thr196, Asp194, and ALA205 in YAP1 form hydrogen bonds with residues Leu325, Arg370, and His385 in KLF4, respectively. The hydrophobic residues Trp177, Leu207, Phe165, and Met163 in YAP1 and the hydrophobic residues Leu325, Phe386, Met391, Met392, and Leu393 in KLF4 form van der Waals forces. The carboxyl group of Asp194 in YAP1 forms an electrostatic force with protonated guanidine Arg370 in KLF4 (Figures 4(f) and 4(g)). Furthermore, the interaction of KLF4 and YAP1 was validated by coimmunoprecipitation (co-IP) experiments in the BGC-823 cells. The overexpression constructs of KLF4 and the control were designated as Flag-KLF4 and GV358. The results showed that KLF4 can interact with YAP1 in the BGC-823 cells with overexpression of Flag-KLF4 compared to the control group (Figure 4(h)).

3.5. UA Inhibited the Growth of Gastric Cancer In Situ in Mice. We have proved that UA inhibited the growth of the BCG-823 cells through activating KLF4 expression. Moreover, we suggested UA can restrain tumor growth in vivo. As a result, we designed a successful orthotopic tumor transplantation model on nude mice (Figure 5(a)). The tumor weight and volume were analyzed, and we found overexpression of KLF4 as well as UA treatment significantly inhibited the growth of tumors in this model (Figures 5(b) and 5(c)). Furthermore, we detected the mRNA expression levels of CTGF and KLF4 in the tumor tissue and found that CTGF was negatively correlated with KLF4 as expected (Figure 5(d)).

4. Discussion

GC is a common malignant tumor which seriously affects people's life and health. The occurrence of cancer is mainly caused by the activation of tumor promoting genes or the inhibition of tumor suppressor genes. Therefore, there is a need to find a key gene that can be used as a target for the treatment of GC. Here, we demonstrated that KLF4 plays a key role in inhibiting the growth of GC and that KLF4 could interact with YAP1 to interrupt the oncogenic transcriptional process. In addition, UA could effectively inhibit the growth of GC by increasing KLF4 expression.

Many studies have shown that KLF4 plays a role of a tumor suppressor gene in many tumors [21, 22]. It has been reported that KLF4 decreased in lung adenocarcinoma [23], colorectal cancer [24], and hepatocellular carcinoma [25]. Moreover, studies have indicated that KLF4 plays a key role in inhibiting tumor growth [26, 27]. In our study, we found that the overexpression of KLF4 can effectively inhibit the proliferation and cell cycle of the BGC-823 cells. Furthermore, the tumor xenograft model showed that overexpression of KLF4 in the BGC-823 cells dramatically inhibited GC growth in nude mice. In addition, to clarify the mechanism of KLF4 inhibiting the growth of GC, we detected the changes of related genes after overexpression of KLF4, and we found that overexpression of KLF4 can decrease the expression of CTGF, which was consistent with the findings by others that KLF4 could decrease the expression of CTGF [28]. Also, we found that the expression of P21 and P27, which were the downstream of CTGF, increased after overexpression of KLF4. High CTGF

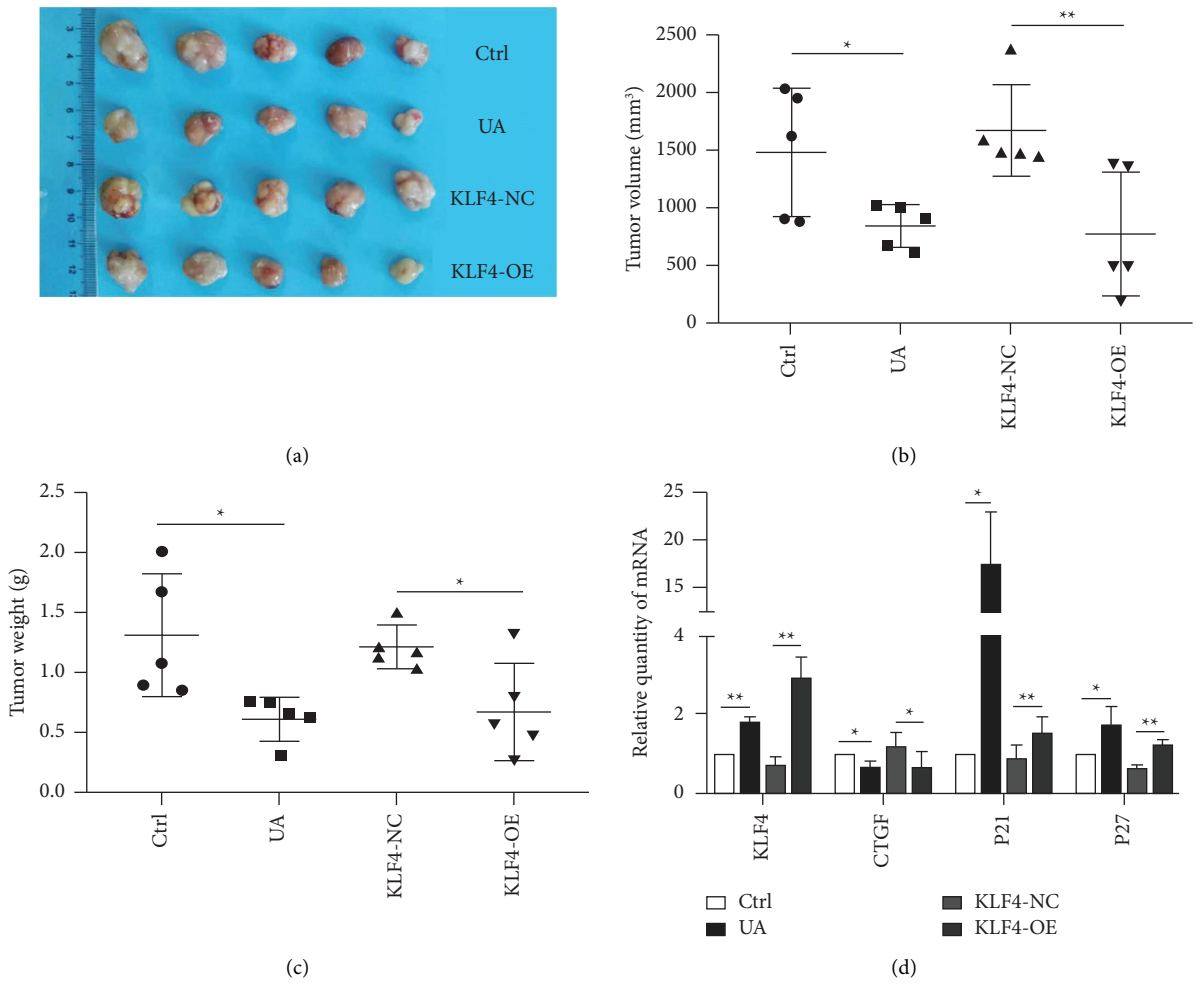

Figure 5: UA inhibited the growth of gastric cancer in situ in mice. (a) Pictures of tumors were taken at the same scale on the 28th day after inoculation. (b) Tumor volume on the 28th day after implantation. (c) Tumor weight on the 28th day after implantation. (d) Real-time PCR analysis of KLF4, CTGF, P21, and P27 mRNA levels extracted from the nude mouse's tumor. $^{*}P < 0.05$, $^{**}P < 0.01$ versus the control group.

expression in tumor tissues was associated with an increased desmoplasia in cancers [29]. Clinical evidence showed upregulation of CTGF correlates with gastric tumor growth, invasion, and poor survival in patients [30, 31]. To confirm the efficacy of CTGF in inhibiting growth in GC cells, we used a lentivirus to achieve the downexpression of CTGF in the BGC-823 cells. We found that after downexpression of CTGF, the proliferation of the BGC-823 cells was inhibited and the cell cycle of BGC-823 cells was blocked in the G2/M stage, and the expression of P21 and P27 increased. The results indicated that the inhibitory effect of KLF4 on GC growth may be fulfilled by CTGF.

CTGF is a typical downstream oncogene of Hippo pathways, which is considered as a therapeutic target of tumors [32]. In order to further clarify how KLF4 affected the expression level of CTGF, we tried to explore the relationship between KLF4 and the Hippo pathway. The core set of Hippo pathways was composed of 4 tumor suppressors, transcriptional coactivator (YAP), and transcriptional factor TEADs [33]. YAP has been identified as a terminal effector of the Hippo pathway because it is the most pivotal step for the core kinase cassette of the pathway [34, 35]. YAP shuttles from the cytoplasm to the nucleus, where it induces the expression of proliferation-promoting and antiapoptotic genes through interaction with TEADs [36, 37]. TEADs are considered key transcription factor partners for YAP in regulation of gene expression. Knockdown of TEADs or disruption of the interaction of YAP-TEADs diminished YAP-dependent gene transcription and oncogenic transformation both in vitro and in vivo [38, 39]. There are WW domains at the N-terminal of YAP, and the WW domains specifically recognize and bind to proline-rich motif [40]. It mediated protein-protein interactions in many cases. TEADs contain an N-terminal TEA DNA-binding domain which contains a "PPXY" sequence that contributes to YAP1 interaction [41]. We analyzed the amino acid sequence and found that KLF4 includes "PPGF" instead of "PPXY." A yeast two-hybrid system proved that KLF4 and YAP1 did combine with each other in vitro. We further used molecular docking to predict the binding sites. Therefore, the WW domains of YAP1 might recognize the "PPGF" sequence as a binding signal as

well. KLF4 may competitively interact with YAP1 protein to block the formation of the YAP1-TEADs complex, which is a novel breakthrough in the Hippo pathway participants in cell growth regulation. To show the interaction of KLF4 to YAP1 in human cells, we performed co-IP experiments. The results showed that KLF4 can interact with YAP1 in the BGC-823 cells which further supported our conclusion. However, it needs more evidence, such as it is important to perform pulldown to prove direct protein-protein interplay and the binding sites between KLF4 and YAP1, and we will demonstrate it in future experiments.

UA is a pentacyclic triterpenoid compound that is derived from a range of medicinal herbs. Several studies have confirmed that UA has antiproliferative properties in a variety of cancer cell lines [42–44]. To investigate the mechanism of UA in inhibiting the growth of GC, we determined the role of UA in regulating the expression of KLF4 and CTGF. We found that UA could significantly increase the expression of KLF4 and decrease the level of CTGF. UA inhibits the growth of GC through regulating KLF4. Similarly, it needs further experiment to support the conclusion, such as it is better to compare the growth inhibitory effect of UA on WT and KLF4-KD cells to show that KLF4 is a target of UA.

In conclusion, although multiple signaling pathways have been demonstrated to be involved in anticancer effects, our results presented here are particularly novel because the data revealed that KLF4 as a tumor suppressor, which interacted with YAP1, negatively inhibited oncogenic gene CTGF. Moreover, we also demonstrated that UA, a natural compound, can block the oncogenic pathway of GC through activating KLF4 both in vivo and in vitro. Our studies may provide novel therapy for GC patients.

Data Availability

The data used and/or analyzed during the current study are available from the corresponding author on reasonable request.

Ethical Approval

All animal experiments were approved and supervised by the Institutional Animal Care and Use Committee of Putuo Hospital, Shanghai University of Traditional Chinese Medicine, P. R. China. All animal studies were conducted in accordance with the National Institute of Health guidelines for the Care and Use of Laboratory Animals.

Conflicts of Interest

The authors declare that they have no conflicts of interest.

Authors' Contributions

XK, RW, and WH conceived and designed the project. WH, FX, and ZC completed the experiments and acquired the data. WH, FX, and MZ wrote the article and prepared the images of the figures. QL, RL, and QG analyzed the data. ZZ and XL revised the manuscript. All the authors read and approved the final version of this manuscript. Fenfen Xiang, Mengzhe Zhang, and Wenbin Hao contributed equally to this work.

Acknowledgments

This research was supported by grants from the One Hundred Talents Project of Putuo Hospital, Shanghai University of Traditional Chinese Medicine (No. 2022-RCQH-03) and the Science Technology Innovation Project of Putuo District Health System (No. ptkwws202307).

References

[1] F. Bray, J. Ferlay, I. Soerjomataram, R. L. Siegel, L. A. Torre, and A. Jemal, "Global cancer statistics 2018: GLOBOCAN estimates of incidence and mortality worldwide for 36 cancers in 185 countries," *Ca-a Cancer Journal for Clinicians*, vol. 68, no. 6, pp. 394–424, 2018.

[2] R. J. Huang, H. Koh, J. H. Hwang, and L. Summit, "A summary of the 2020 gastric cancer summit at stanford university," *Gastroenterology*, vol. 159, no. 4, pp. 1221–1226, 2020.

[3] T. Fujita, "Targeted therapy for gastric cancer," *The Lancet Oncology*, vol. 14, no. 6, pp. 440–442, 2013.

[4] J. Wang, C. Li, X. Zhu, and J. Zhu, "Adjuvant therapy in resectable gastric cancer-the CRITICS trial," *The Lancet Oncology*, vol. 19, no. 7, p. e330, 2018.

[5] J. Zhang, Z. Zhu, H. Wu et al., "PODXL, negatively regulated by KLF4, promotes the EMT and metastasis and serves as a novel prognostic indicator of gastric cancer," *Gastric Cancer*, vol. 22, no. 1, pp. 48–59, 2019.

[6] F. Kong, T. Sun, X. Kong, D. Xie, Z. Li, and K. Xie, "Kruppel-like factor 4 suppresses serine/threonine kinase 33 activation and metastasis of gastric cancer through reversing epithelial-mesenchymal transition," *Clinical Cancer Research*, vol. 24, no. 10, pp. 2440–2451, 2018.

[7] T. Yu, X. Chen, T. Lin et al., "KLF4 deletion alters gastric cell lineage and induces MUC2 expression," *Cell Death & Disease*, vol. 7, no. 6, Article ID e2255, 2016.

[8] H. He, S. Li, Y. Hong et al., "Kruppel-like factor 4 promotes esophageal squamous cell carcinoma differentiation by up-regulating keratin 13 expression," *Journal of Biological Chemistry*, vol. 290, no. 21, pp. 13567–13577, 2015.

[9] Z. Liu, H. Yang, W. Luo et al., "Loss of cytoplasmic KLF4 expression is correlated with the progression and poor prognosis of nasopharyngeal carcinoma," *Histopathology*, vol. 63, no. 3, pp. 362–370, 2013.

[10] M. He, Z. Chen, M. Martin et al., "miR-483 targeting of CTGF suppresses endothelial-to-mesenchymal transition: therapeutic implications in kawasaki disease," *Circulation Research*, vol. 120, no. 2, pp. 354–365, 2017.

[11] J. K. Holden and C. N. Cunningham, "Targeting the hippo pathway and cancer through the TEAD family of transcription factors," *Cancers*, vol. 10, no. 3, 2018.

[12] W. Kang, A. S. Cheng, J. Yu, and K. F. To, "Emerging role of Hippo pathway in gastric and other gastrointestinal cancers," *World Journal of Gastroenterology*, vol. 22, no. 3, pp. 1279–1288, 2016.

[13] Z. Fan, H. Xia, H. Xu et al., "Standard CD44 modulates YAP1 through a positive feedback loop in hepatocellular carcinoma," *Biomedicine & Pharmacotherapy*, vol. 103, pp. 147–156, 2018.

[14] D. Sun, X. Li, Y. He et al., "YAP1 enhances cell proliferation, migration, and invasion of gastric cancer in vitro and in vivo," *Oncotarget*, vol. 7, no. 49, pp. 81062–81076, 2016.

[15] W. Kang, T. Huang, Y. Zhou et al., "miR-375 is involved in Hippo pathway by targeting YAP1/TEAD4-CTGF axis in gastric carcinogenesis," *Cell Death & Disease*, vol. 9, no. 2, p. 92, 2018.

[16] S. H. Kim, H. Jin, R. Y. Meng et al., "Activating hippo pathway via rassf1 by ursolic acid suppresses the tumorigenesis of gastric cancer," *International Journal of Molecular Sciences*, vol. 20, no. 19, 2019.

[17] A. M. Mancha-Ramirez and T. J. Slaga, "Ursolic acid and chronic disease: an overview of UA's effects on prevention and treatment of obesity and cancer," *Advances in Experimental Medicine and Biology*, vol. 928, pp. 75–96, 2016.

[18] J. Lin, Y. Chen, L. Wei, Z. Hong, T. J. Sferra, and J. Peng, "Ursolic acid inhibits colorectal cancer angiogenesis through suppression of multiple signaling pathways," *International Journal of Oncology*, vol. 43, no. 5, pp. 1666–1674, 2013.

[19] F. Xiang, Y. Fan, Z. Ni et al., "Ursolic acid reverses the chemoresistance of breast cancer cells to paclitaxel by targeting MiRNA-149-5p/MyD88," *Frontiers Oncology*, vol. 9, p. 501, 2019.

[20] F. Xiang, Z. Zhu, M. Zhang et al., "3,3'-Diindolylmethane enhances paclitaxel sensitivity by suppressing DNMT1-mediated KLF4 methylation in breast cancer," *Frontiers Oncology*, vol. 11, Article ID 627856, 2021.

[21] K. Guo, J. Cui, M. Quan et al., "The novel KLF4/MSI2 signaling pathway regulates growth and metastasis of pancreatic cancer," *Clinical Cancer Research*, vol. 23, no. 3, pp. 687–696, 2017.

[22] M. Shi, J. Cui, J. Du et al., "A novel KLF4/LDHA signaling pathway regulates aerobic glycolysis in and progression of pancreatic cancer," *Clinical Cancer Research*, vol. 20, no. 16, pp. 4370–4380, 2014.

[23] T. Ma, B. Yan, Y. Hu, and Q. Zhang, "HOXA10 promotion of HDAC1 underpins the development of lung adenocarcinoma through the DNMT1-KLF4 axis," *Journal of Experimental & Clinical Cancer Research*, vol. 40, no. 1, p. 71, 2021.

[24] N. V. Patel, A. M. Ghaleb, M. O. Nandan, and V. W. Yang, "Expression of the tumor suppressor Kruppel-like factor 4 as a prognostic predictor for colon cancer," *Cancer Epidemiology, Biomarkers & Prevention*, vol. 19, no. 10, pp. 2631–2638, 2010.

[25] Q. Li, Y. Gao, Z. Jia et al., "Dysregulated Kruppel-like factor 4 and vitamin D receptor signaling contribute to progression of hepatocellular carcinoma," *Gastroenterology*, vol. 143, no. 3, pp. 799–810 e792, 2012.

[26] Y. Ou, H. Ren, R. Zhao et al., "*Helicobacter pylori* CagA promotes the malignant transformation of gastric mucosal epithelial cells through the dysregulation of the miR-155/KLF4 signaling pathway," *Molecular Carcinogenesis*, vol. 58, no. 8, pp. 1427–1437, 2019.

[27] V. W. Yang, Y. Liu, J. Kim, K. R. Shroyer, and A. B. Bialkowska, "Increased genetic instability and accelerated progression of colitis-associated colorectal cancer through intestinal epithelium-specific deletion of Klf4," *Molecular Cancer Research*, vol. 17, no. 1, pp. 165–176, 2019.

[28] Y. An, B. Xu, G. Yan, N. Wang, Z. Yang, and M. Sun, "YAP derived circ-LECRC functions as a brake signal to suppress hyperactivation of oncogenic YAP signalling in colorectal cancer," *Cancer Letters*, vol. 532, Article ID 215589, 2022.

[29] A. Mazzocca, E. Fransvea, F. Dituri, L. Lupo, S. Antonaci, and G. Giannelli, "Down-regulation of connective tissue growth factor by inhibition of transforming growth factor beta blocks the tumor-stroma cross-talk and tumor progression in hepatocellular carcinoma," *Hepatology*, vol. 51, no. 2, pp. 523–534, 2010.

[30] C. G. Jiang, L. Lv, F. R. Liu et al., "Downregulation of connective tissue growth factor inhibits the growth and invasion of gastric cancer cells and attenuates peritoneal dissemination," *Molecular Cancer*, vol. 10, p. 122, 2011.

[31] Z. Liu, J. Li, Y. Ding et al., "USP49 mediates tumor progression and poor prognosis through a YAP1-dependent feedback loop in gastric cancer," *Oncogene*, vol. 41, no. 18, pp. 2555–2570, 2022.

[32] Y. Zhou, J. Zhang, H. Li et al., "AMOTL1 enhances YAP1 stability and promotes YAP1-driven gastric oncogenesis," *Oncogene*, vol. 39, no. 22, pp. 4375–4389, 2020.

[33] J. Huang, S. Wu, J. Barrera, K. Matthews, and D. Pan, "The Hippo signaling pathway coordinately regulates cell proliferation and apoptosis by inactivating Yorkie, the Drosophila Homolog of YAP," *Cell*, vol. 122, no. 3, pp. 421–434, 2005.

[34] M. Sudol, D. C. Shields, and A. Farooq, "Structures of YAP protein domains reveal promising targets for development of new cancer drugs," *Seminars in Cell & Developmental Biology*, vol. 23, no. 7, pp. 827–833, 2012.

[35] D. Pan, "The hippo signaling pathway in development and cancer," *Developmental Cell*, vol. 19, no. 4, pp. 491–505, 2010.

[36] C. Webb, A. Upadhyay, F. Giuntini et al., "Structural features and ligand binding properties of tandem WW domains from YAP and TAZ, nuclear effectors of the Hippo pathway," *Biochemistry*, vol. 50, no. 16, pp. 3300–3309, 2011.

[37] K. C. Lin, H. W. Park, and K. L. Guan, "Regulation of the hippo pathway transcription factor TEAD," *Trends in Biochemical Sciences*, vol. 42, no. 11, pp. 862–872, 2017.

[38] B. Zhao, L. Li, Q. Lei, and K. L. Guan, "The Hippo-YAP pathway in organ size control and tumorigenesis: an updated version," *Genes & Development*, vol. 24, no. 9, pp. 862–874, 2010.

[39] B. Zhao, X. Ye, J. Yu et al., "TEAD mediates YAP-dependent gene induction and growth control," *Genes & Development*, vol. 22, no. 14, pp. 1962–1971, 2008.

[40] M. Imajo, M. Ebisuya, and E. Nishida, "Dual role of YAP and TAZ in renewal of the intestinal epithelium," *Nature Cell Biology*, vol. 17, no. 1, pp. 7–19, 2015.

[41] Y. Ma, Y. Yang, F. Wang, Q. Wei, and H. Qin, "Hippo-YAP signaling pathway: a new paradigm for cancer therapy," *International Journal of Cancer*, vol. 137, no. 10, pp. 2275–2286, 2015.

[42] J. H. Kim, Y. H. Kim, G. Y. Song et al., "Ursolic acid and its natural derivative corosolic acid suppress the proliferation of APC-mutated colon cancer cells through promotion of beta-catenin degradation," *Food and Chemical Toxicology*, vol. 67, pp. 87–95, 2014.

[43] Y. L. Hsu, P. L. Kuo, and C. C. Lin, "Proliferative inhibition, cell-cycle dysregulation, and induction of apoptosis by ursolic acid in human non-small cell lung cancer A549 cells," *Life Sciences*, vol. 75, no. 19, pp. 2303–2316, 2004.

[44] K. A. Manu and G. Kuttan, "Ursolic acid induces apoptosis by activating p53 and caspase-3 gene expressions and suppressing NF-kappaB mediated activation of bcl-2 in B16F-10 melanoma cells," *International Immunopharmacology*, vol. 8, no. 7, pp. 974–981, 2008.